# Photoemission studies of sulfur

Paul Nielsen
*Xerox Webster Research Center, Webster, New York 14580*
(Received 19 March 1974)

Photoemission measurements on polycrystalline orthorhombic sulfur films and glassy films of $S_8$ molecules have been made at various photon energies up to 21.2 eV. There is essentially no difference in the densities of states of the polycrystalline and glassy films. The four peaks found agree in both amplitude and location with an adjusted semiempirical molecular-orbital calculation of the $S_8$ molecule made by Chen. A deeper-lying broad peak which has been found in all the chalcogens at x-ray energies and attributed to $s$-like electrons is not observed at 21.2-eV photon energy; it is argued that further calculations are required to justify association of this deep x-ray peak with the $s$ electrons. The density of occupied states is completely different from that assumed by Cook and Spear to explain their optical data, but their $\epsilon_2(E)$ curve can also be reproduced moderately well by the present results.

## I. INTRODUCTION

Orthorhombic sulfur, composed of $S_8$ puckered-ring molecules, is one of the simplest of molecular crystals. Because of this relative simplicity, a complete understanding of its electronic and optical properties may be expected to be easier to achieve than in more complicated molecular crystals; at the same time such understanding should provide a useful guide to more complex systems. But curiously, orthorhombic sulfur has received less attention than many more complex organic molecular crystals.

Cook and Spear[1] have investigated the optical reflectivity in the 2.5–14-eV range and presented a Kramers-Kronig analysis to determine $\epsilon_1(\omega)$ and $\epsilon_2(\omega)$. Hellyer[2] and Komp and Fitzsimmons[3] made measurements of the total vacuum photoemission yield; however, only Hellyer's measurements extend more than 2 eV above the ionization threshold and his value of $E_T$ disagrees with that of Komp and Fitzsimmons. Chen[4] has made the only complete semiempirical molecular-orbital calculations of the $S_8$ molecule and of electronic states in the solid,[5] although Gibbons (unpublished work cited in Ref. 1, see also Ref. 29) earlier analyzed the $S_8$ ring in terms of unmixed $\sigma$ and $\pi$ orbitals. More recently, Dalrymple and Spear[6] have compared the optical properties of monoclinic Se and orthorhombic S and proposed electronic energy band structures based on Gibbon's analysis.

Both Chen and Gibbons assumed that $s$-$p$ hybridization was required to explain the S-S bond angle of 107.9° in the $S_8$ ring, and Chen determined the extent of hybridization from the measured bond angle. However, Kastner[7] argued that hybridization was not necessary in the chalcogens. He proposed instead that the valence band should consist of two $p$ electrons in a lone pair and two in bonding states with the two nearest neighbors, while the two $s$ electrons would form a deeper isolated atomiclike level. Photoemission measurements of Nielsen[8] found no trace of the separate $s$ electrons of amorphous Se, and indeed Chen[9] was able to obtain very good agreement with those measurements using a semiempirical calculation similar to the one for S. On the other hand, x-ray photoemission measurements of Pollack *et al.*[10] and Shevchik *et al.*[11] on Te, and Te and Se, respectively, revealed a deeper valence peak which was attributed to unhybridized $s$ electrons. Knowledge of the density of states in sulfur may help to resolve this controversy about the density of electronic states in the chalcogens. The only relatively direct determination that has been reported is that of Gusatinskii and Nemnonov,[12] who combined x-ray emission data on various unspecified forms of sulfur to obtain a density of valence electron states which bears little resemblance to that deduced by Dalrymple and Spear.

Vacuum photoemission combined with kinetic-energy determination of the emitted electrons allows one to determine the initial state from which the electron is excited, and in consequence it is possible in many cases to determine directly the density of states in the solid. In this paper I will describe in Sec. II the experimental methods used to investigate sulfur by vacuum photoemission. A description and analysis of the results will be given in Sec. III. In Sec. IV comparison with calculations of Chen and other measurements of optical and electronic properties will be made. Also, these results on sulfur will be related to the measurements on Se and Te which have been reported. Finally, the implications for the question of $s$-$p$ hybridization will be discussed.

## II. EXPERIMENTAL METHOD

### A. Apparatus

The photoemission system used in this investigation is essentially the same as that previously

described.[8] A McPherson 218 vacuum monochromator with $H_2$ discharge lamp and a windowless, differentially pumped lamp using He or Ne are used to provide 7.7–10.8-eV, and 21.2- or 16.85-eV photons, respectively. A photomultiplier tube and sodium-salicylate-coated screen are used to monitor the photon flux in the 7.7–10.8-eV range. Energy analysis is provided by a 7.5-cm-diam screen surrounding the emitter, which has applied to it a slowly swept ramp voltage and a 3-Hz, 0.15-V peak-to-peak, modulation voltage. The modulated emitted photocurrent is amplified with a virtual-ground current preamplifier and then converted to dc with a lock-in amplifier. The resolution of the energy analyzer, $E_{res}$, is 0.15 V full width at half-maximum. The ion-pumped vacuum chamber has a base pressure of $\sim 10^{-10}$ torr after bakeout, although in these studies of sulfur the pressure was generally higher, as discussed below.

Because sulfur has a relatively high vapor pressure at room temperature it was necessary to provide for sample cooling below ambient, while at the same time maintaining the good electrical insulation of the emitter structure required to measure the emitted current, and allowing for rotation of any one of four emitters set 90° apart into the analyzer screen. This was accomplished by a BeO insulating wafer and straps of copper braid to permit simultaneous sample cooling and rotation. With liquid nitrogen as the coolant an emitter temperature of about 100 K could be reached. Alternatively a temperature of about −18 °C was provided by using ethanol circulated through an ethanol–dry-ice bath.

### B. Preparation of sulfur films

The vapor pressure of sulfur is $10^{-5}$ torr at 18 °C and $10^{-7}$ torr at −17 °C.[13] Consequently, the rate of evaporation at room temperature (~22 °C) is too high to permit measurements on evaporated films, and the emitter must be cooled. The high vapor pressure also makes it impractical to bake the portion of the ultrahigh-vacuum (UHV) chamber containing the sulfur source, but chamber pressures in the $10^{-9}$-torr range could be obtained by allowing a longer pumping period than usual, and a pressure near $10^{-10}$ torr was reached after baking all of the UHV system except the experimental chamber. Although the chamber pressure was higher than is desirable in photoemission work, the sample was self-cleaning when cooled only to −18 °C since the rate of reevaporation of sulfur was ten or more times the rate at which residual gas impacted it. Even when cooled to 100 K there were no changes in the photoemission energy distribution curves (EDCs) indicative of significant contamination.

Films of sulfur composed of $S_8$ molecules were prepared by sublimation of chips of high-purity natural crystals of orthorhombic sulfur[14] contained in a resistance-heated quartz crucible. Deposits were generally at a rate of about 5–10 Å $sec^{-1}$. It is known that the vapor above subliming orthorhombic sulfur contains less than 1% of species other than the $S_8$ ring.[15] Consequently, since the orthorhombic form of sulfur is the stable modification below 95.5 °C,[16] the films prepared by deposition on cooled substrates must be either a noncrystalline aggregate of $S_8$ rings, or crystallites of orthorhombic sulfur. In fact, sulfur deposited on air-oxidized polished aluminum substrates at −18 °C was always polycrystalline, while deposits on clean gold films at −18 °C or deposits on either gold or oxidized Al at ~100 K were visually glassy. No x-ray- or electron-diffraction measurements could be made on the glassy films, but it appears unlikely that those prepared on ~100-K substrates were crystalline.

In order to minimize the development of surface charge on the films during measurement the thickness had to be kept small. At −18 °C a thickness of 1000–2000 Å was sufficient to suppress all photoelectrons from the substrate while keeping the energy shift due to surface charging below 0.1 eV. The films on substrates cooled to ~100 K had much lower conductivity and the thickness had to be kept below a few hundred angstroms to prevent surface charging. These films gave more uniform coverage than those prepared on substrates at −18 °C and no photoemission from the substrates was observed. Film thicknesses were determined approximately with a quartz crystal monitor at room temperature and may be underestimates; however, once the films on 100-K substrates became visible through the development of interference colors they were highly insulating.

## III. RESULTS

### A. 16.85- and 21.2-eV photon energy

Energy distribution curves (EDCs) of polycrystalline orthorhombic sulfur at 21.2- and 16.85-eV photon energies are shown in Fig. 1. The $S_8$ vapor was condensed on an oxidized aluminum substrate held at −18 °C and produced a polycrystalline diffusely scattering film. For convenience in later analysis the energy axis gives the initial energy of the photoemitted electrons relative to the Fermi level of the substrate. The energy of the valence-band maximum below the Fermi level is then obtained directly from the high-energy cutoff of the EDC ($E_V$). In these curves $E_V = -3.5$ eV. The EDC is broadened by the analyzer resolution $E_{res}$, so the low-energy cutoff lies at an energy $E_m$ below $E_F$, where

$$E_m = \phi - h\nu - E_{res}, \tag{1}$$

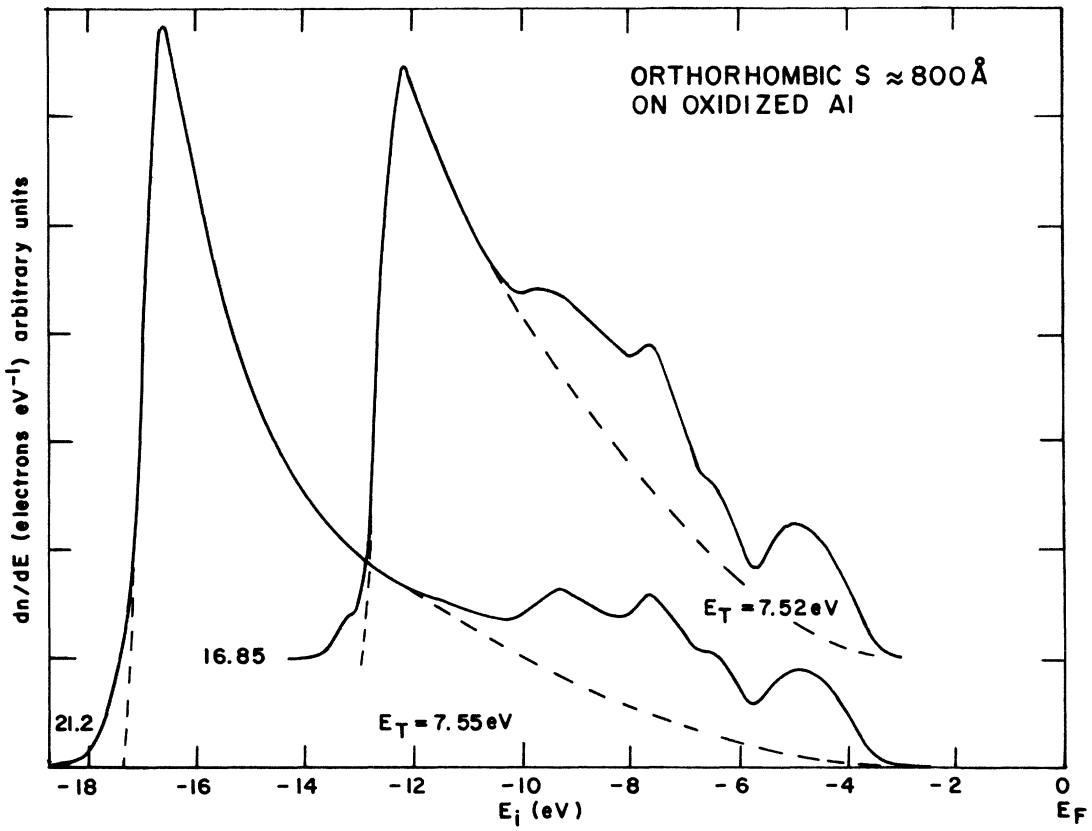


FIG. 1. 16.85- and 21.2-eV EDCS of a polycrystalline orthorhombic sulfur film deposited on an oxidized-Al substrate. The abscissa gives the initial energy from which the electrons were excited, relative to the substrate Fermi energy.

$\phi$ being the work function. The threshold energy $E_T$ is therefore given by

$$E_T = \phi - E_V = E_m + h\nu + E_{res} - E_V . \quad (2)$$

In these curves the low-energy cutoff is distorted because of the polycrystalline and relatively rough surface and so an extrapolation from the steeper part of the curve was made to obtain $E_m$. The threshold energy obtained using Eq. (2) is $E_T = 7.5 \pm 0.1$ eV. Electrons scattered by various inelastic processes are shifted from higher energy into the large low-energy inelastic scattering peak. This large peak in the EDCs cannot be fitted satisfactorily with the calculation of Berglund and Spicer[17] modified for a finite energy gap, contrary to results for amorphous Se (Ref. 8); the dashed lines under the upper parts of the curves are merely plausible extrapolations of the peak. The portion of the experimental curve lying above this extrapolation is related to the occupied density of states. In this figure it is evident that the peak positions and amplitudes are essentially the same at both 16.85- and 21.2-eV photon energy.

Energy distribution curves obtained from a glassy film of $S_8$ condensed on gold at $-18$ °C are shown in Fig. 2. These EDCs are identical with those obtained from (thinner) films prepared at ~100 K. Comparing with Fig. 1, one sees that the low-energy cutoff has become sharp now that the film is smooth. The relative amplitudes of scattering peak and higher-energy structure are about the same for the two kinds of film, but the total number of scattered electrons from the glassy film is much less. A shoulder appears on the upper edge of the scattering peaks at both 16.85- and 21.2-eV photon energy, 1.4 eV above the low-energy cutoff of both curves. This shoulder is not due to lower-energy photons from the lamp and must be a characteristic of the electron distribution emitted from glassy $S_8$ films. There is a very weak peak at about $-12$ eV on the 21.2-eV curve; its magnitude varies somewhat from sample to sample. The higher-energy structure superimposed on the scattering background is essentially the same at both photon energies; it is somewhat sharper than that in Fig. 1, and the amplitude of the uppermost peak relative to the lower ones is greater, as reduced inelastic scattering would lead one to expect. But there are no major differences between the higher-energy structures of the polycrystalline and the

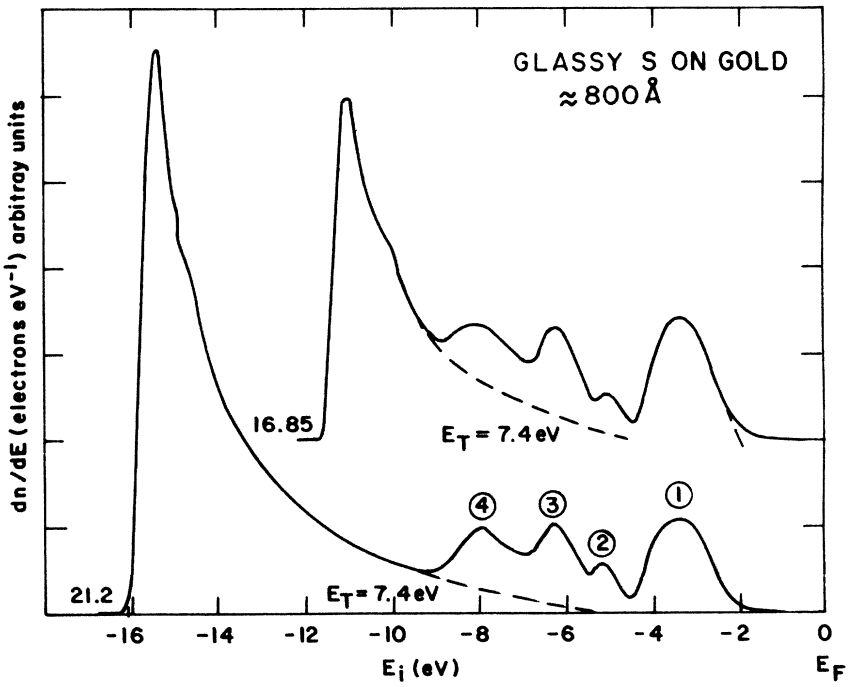


FIG. 2. EDCs of a glassy $S_8$ film deposited on a gold substrate at 16.85- and 21.2-eV photon energy. The low-energy shoulder has been somewhat accentuated in the figure to make it clear.

glassy $S_8$ films.

It should be noted that the valence-band maximum of the film on gold lies 2–2.1 eV below the Fermi level while that of the film on oxidized aluminum is 3.5 eV below $E_F$. This difference remains when the substrates are made colder so that both films are glassy. Since the work function of the gold film is about 5.2 eV while that of the oxidized aluminum is about 4 eV it is evident that the sulfur band maximum lies about 7.5 eV below the substrate vacuum level. This indicates that the vacuum level of the sulfur film is in nearly perfect alignment with that of the substrate.

### B. 7.7–10.8-eV photon energy

To study the upper part of the valence band of sulfur in more detail lower photon energies are necessary. Figure 3 gives a family of curves at different photon energies normalized to the same incident photon flux. The $S_8$ vapor was condensed on a gold substrate at 100 K and to reduce charging effects a white-light microscope illuminator was directed on the sample during the measurements. In this case the gold surface had been previously exposed to air and its work function was reduced to 4.9 eV from the 5.2 eV of a clean surface. Consequently, the valence-band maximum should have dropped 0.3 eV, and actually dropped slightly more.

At 10.78 eV there is a small shoulder on the low-energy edge which corresponds to the minimum between peaks 2 and 3 of Fig. 2. The low-energy peak corresponds to peak 2 while the high-energy peak is peak 1. These peaks are separated by 1.8 eV just as in Fig. 2; however, peak 2 is relatively much larger than at higher photon energy. When the photon energy is reduced to 10.2 eV the amplitude of peak 2 is considerably reduced but the upper peak is almost unchanged. The upper peak gradually changes shape as the photon energy is reduced from 10.2 eV.

A short bar has been placed at the low-energy cutoff of the 10.78-eV curve. Similar bars are then placed on the other curves shifted by the photon energy difference from 10.78 eV. It then becomes evident that the 9.72-eV curve actually falls completely to zero, because of the minimum between peaks 1 and 2, before the low-energy cutoff at zero electron kinetic energy is expected.

EDCs of polycrystalline films in this energy range are similar to Fig. 3, but contain less detail. The variation in amplitude of peak 2 with photon energy occurs in the same way for polycrystalline as for glassy films.

### C. Low-kinetic-energy region

It has already been remarked that peak 2 seems much larger in the 10.78-eV curve than at 21.2 eV. Further examination of the curves of Fig. 3 suggests that the upper portion of peak 1 is enhanced when the electron kinetic energy is about 0.6 eV. To clarify this feature the ratio $F_{\hbar\omega}(E, E_i)/F_{21.2}(E_i)$ is given for different photon energies in

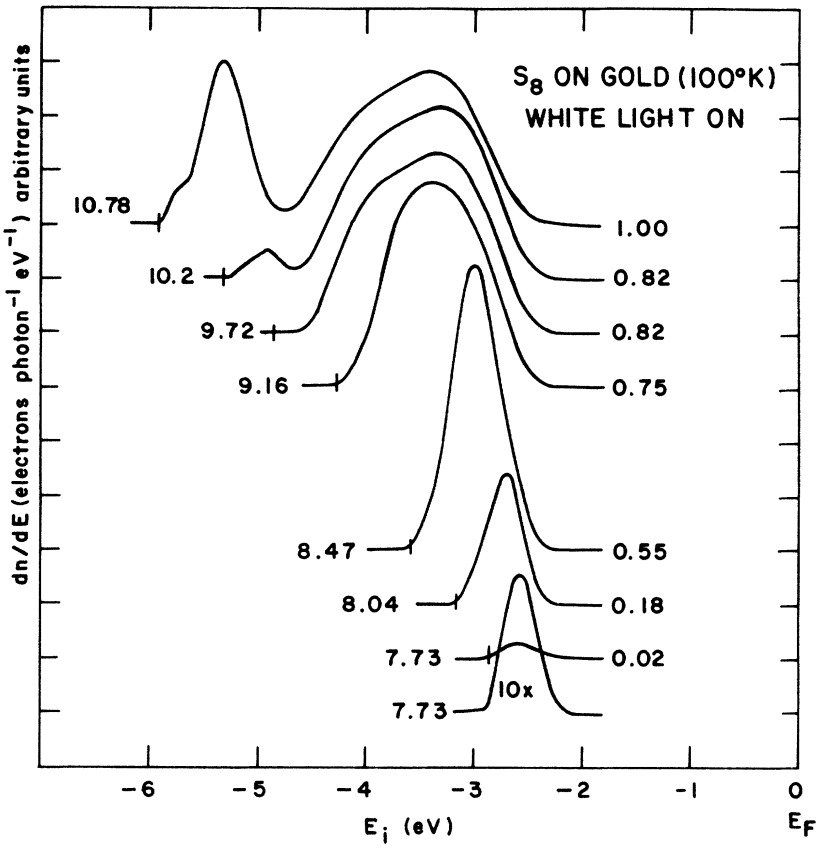


FIG. 3. EDCs of a glassy $S_8$ film at 7.73–10.78-eV photon energy. All curves are normalized to the same arbitrary incident photon flux and the numbers at the right-hand end give the total yield normalized to the 10.78-eV curve. A white microscope illuminator was used to prevent sample charging.

Fig. 4. $F_{\hbar\omega}(E, E_i)$ is the amplitude of the EDC at photon energy $\hbar\omega$, electron kinetic energy $E$ above zero, and initial energy $E_i$; $F_{21.2}$-eV curve at the same initial energy $E_i$. This ratio of EDC amplitudes at the same initial-state energy but different photon energies largely suppresses structure in the initial density of states and brings out differences due to the energy dependence of the transition matrix element, structure in the density of final states, and the threshold function. In the nondirect-transition model of photoemission,[17] initial-density-of-states structure is completely absent from this ratio.

It is clear from this figure that there is indeed a very strong enhancement in the EDCs at an electron kinetic energy of 0.7 eV and that this enhancement is not present at $h\nu = 9.72$ eV. The rapid drop of the amplitude ratio at high final-state energy is of no significance. It arises from greater instrumental tailing above the valence-band maximun in the 21.2 eV EDC than in the lower-energy EDCs, so that the ratio of these two small amplitudes decreases rather than remaining constant. Because the photon flux at 21.2 eV was not determined relative to that at the lower photon energies, the magnitude of the ratio is arbitrary.

## IV. DISCUSSION

### A. Effect of crystallinity

Because the polycrystalline and glassy films of $S_8$ rings have essentially the same EDC structure we conclude that the electronic structure of the $S_8$ molecule is relatively insensitive to the precise environment of the ring. This is in accord with the weak bonding between rings in the solid, which is evident experimentally in the high vapor pressure of the solid. On the theoretical side Chen[5] has calculated that the intermolecular energy integrals for orthorhombic sulfur are all less than 0.36 eV, and most are much less. In consequence, the bands are mostly only about 0.6 eV wide.

Insensitivity of the $S_8$ electronic structure to the disposition of the rings in the solid implies that the EDC structure which is observed should be closely related to the electronic density of states of the free molecule. In order to make a comparison between the electronic structure of the solid and that of the molecule it should only be necessary to include the effect of the polarization of the solid around the hole left behind when an electron is removed from a filled level, and around any electrons added to empty molecular orbitals.[18] In the following it will be assumed that this polarization

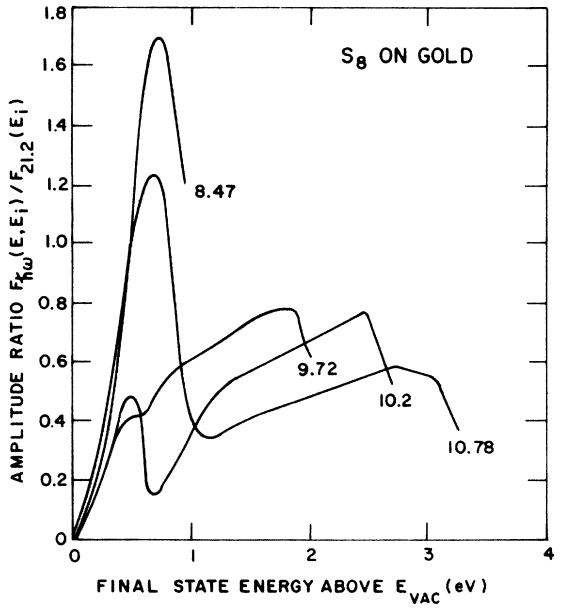


FIG. 4. Plot of the amplitude ratio (see text) as a function of final-state energy for the glassy $S_8$ films.

effect is the same for all filled orbitals, and hence that it leads only to a constant energy shift for all orbitals.

### B. Density of occupied states

The interpretation of photoemission data according to the semiclassical three-step model[17] has generally given reasonable agreement with calculated band structures, and that model will be followed here. Photoemission is imagined to consist of the three steps of excitation, transport to the surface, and escape over the surface barrier into vacuum. A reasonably good first approximation in the case of semiconductors is to equate the transport and escape steps to a step function at the vacuum level[8] and to suppose that the measured EDC is a replica of the distribution of excited electrons within the solid, augmented by a low-energy peak due to inelastically scattered electrons. In the present case [contrary to amorphous Se (Ref. 8)] the inelastic scattering peak in the EDCs of Figs. 1 and 2 cannot be fitted by the simple calculation[17]; the inelastic contribution to the upper part of the EDC has been estimated by a curve fitted to the lower part. Relatively little error can be introduced in the densities of states obtained from Fig. 2 by this procedure.

There are two ways in which the electron energy distribution in the solid may be related to the electronic densities of states. Most simply, it may be assumed that the photoinduced transitions are not restricted by any selection rules, in which case the excited-electron distribution is just the product of initial and final densities of states and a constant transition probability. Or it may be necessary to take into account selection rules arising from $k$ conservation or, in the present case, molecular symmetry, and energy dependence of the transition probability. Because high-energy excited states must be broadened considerably according to the Heisenberg uncertainty relation (lifetime broadening), structure arising from the final density of states, or the dependence of the transition probability on the symmetry of the final state, will be most evident at low photon energy, and hence low electron kinetic energy. We have seen in Figs. 1 and 2 that the 21.2- and 16.85-eV-photon-energy EDCs have identical structures in the upper part of the distribution. Consequently, there is no modulation of the excited-electron distribution by the changed photon energy and these EDCs should give the initial (valence-band) density of states directly.

However, at the low-kinetic-energy end of the EDC there is structure which depends on photon energy, as shown in Fig. 4. Because these ratio curves depend on photon energy, the structure in the EDCs at about 0.7 eV cannot be due simply to a peak in the final density of states or the threshold function 0.7 eV above the vacuum level, which would produce an effect independent of photon energy. Instead, the structure must be due to the combined effect of a peak in the final density of states about 0.7 eV above the vacuum level, or 8.2 eV above the valence-band maximum, and a dip in the transition probability for excitation to this final state peak from states in the lower part of peak 1 (at $-4$ eV in Fig. 3).

Because Chen[4] has made the only complete calculation of the molecular orbitals and energies of the $S_8$-ring molecule, comparison of his calculation with the experimental density of states obtained from the high-photon-energy EDC's appears most useful. The molecular orbitals were determined using the semiempirical extended Huckel-molecular-orbital method. The $3s$ and $3p$ atomic orbitals of sulfur were hybridized into two directed bond orbitals and two equivalent lone-pair orbitals, with the degree of hybridization determined by the S-S bond angle. The molecular orbitals were formed by linear combinations of the hybrid orbitals according to the molecular symmetry, and the various overlap integrals were calculated. To obtain the orbital energies the diagonal elements $H_{ii}$ of the Hamiltonian were approximated by the valence-state ionization energies of the atom and the off-diagonal elements $H_{ij}$ by

$$H_{ij} = \tfrac{1}{2} F S_{ij}(H_{ii} + H_{jj}) , \qquad (3)$$

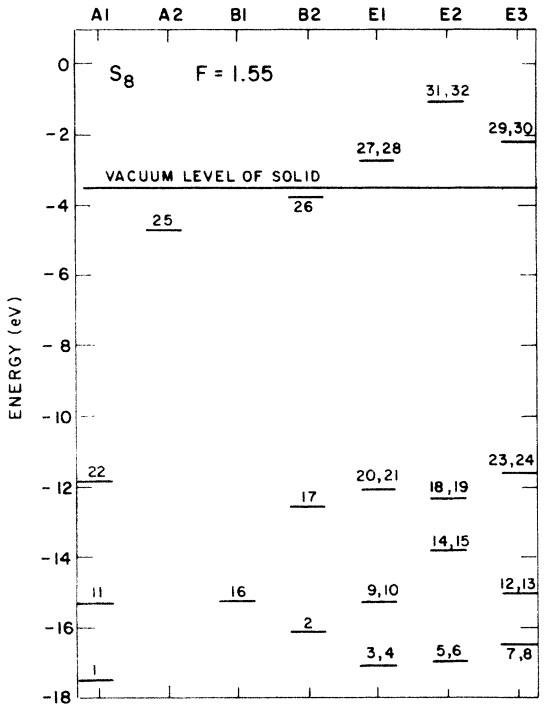


FIG. 5. Orbital energy levels obtained by Chen for the $S_8$ molecules assuming $F = 1.55$. The numbers give the relative ordering of the corresponding orbitals obtained with $F = 2 - |S_{ij}|$ and the orbitals are classified according to their symmetry group (see Ref. 4).

where $S_{ij}$ is an overlap integral between hybrid orbitals and $F$ is a multiplicative factor between 1 and 2. In Ref. 4 the choice

$$F = 2 - |S_{ij}| \tag{4}$$

was made, but Chen also made calculations (unpublished) with various constant values of $F$. He found that the choice of Eq. (4) gave essentially the same occupied orbital energies, but appreciably lower unoccupied orbital energies, than those obtained with a constant $F$ intermediate in value between the maximum and minimum values of $F$ obtained from Eq. (4). Reduction in the value of $F$ reduces the energy range over which the occupied and the empty orbitals are distributed but increases the spacing between these two groups.

It is apparent by inspection that the total spread of the occupied orbitals calculated[4] using Eq. (4) is much greater than the observed valence bandwidth. Of the various constant values considered by Chen, the one which gives the best fit between the calculated and measured valence bandwidths is $F = 1.55$; the energy levels he obtained in this case are shown in Fig. 5 for reference.

To compare the calculated energy levels with the experimental density of states it is convenient to broaden each calculated level by a Gaussian function of width $W$, and then take the sum of the Gaussians. In Fig. 6, the excess of the 21.2-eV EDC of Fig. 2 above the inelastic scattering peak is compared with densities of states obtained in this way from Chen's calculations. The energy axis used gives energy below the valence-band maximum for both theoretical and experimental curves. The amplitude of the experimental curve was normalized at peak 1 to the $F = 1.55$ theoretical curve. A Gaussian width of 0.6 eV was used for best agreement between experiment and theory. It is evident that the calculation with $F = 2 - |S_{ij}|$ does not agree with the experiment but that the density of states calculated with $F = 1.55$ agrees extremely well. Even the Gaussian width of 0.6 eV is in reasonable accord with the calculated broadening of the energy levels in the crystal. The only noticeable fault is that peak 1 is slightly narrower than the experimental peak.

Agreement between experiment and calculation is marred only by the fact, evident from Fig. 5, that the calculated spacing between occupied and empty orbitals is much larger than the optical-absorption gap of about 4 eV. However, a noncon-

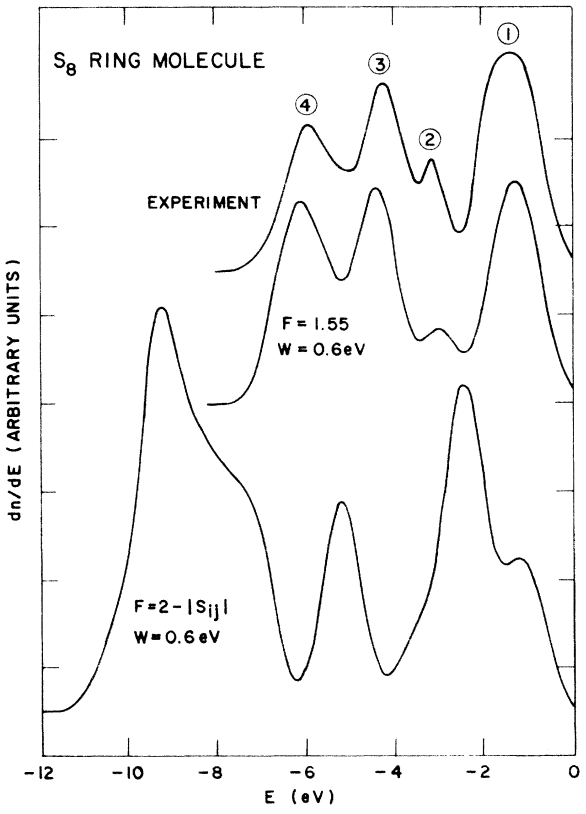


FIG. 6. Comparison of the experimental density of valence states of $S_8$, with calculated densities obtained with the values of 1.55 and $2 - |S_{ij}|$ for the parameter $F$.

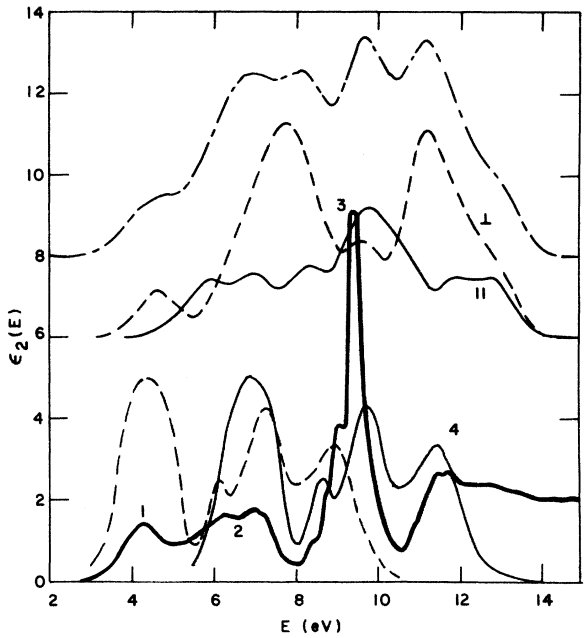


FIG. 7. Heavy solid line gives the experimental curve for $\epsilon_2(E)$ (Cook and Spear). The lower dashed and solid curves give the two parts of a calculation of $\epsilon_2(E)$ based on the photoemission density of valence states (see text). The upper curves (displaced) give the parallel (solid) and perpendicular (dashed) polarization $\epsilon_2(E)$ obtained from the MO calculation and molecular selection rules; the dot-dashed curve gives $\epsilon_2(E)$ assuming no selection rules apply to the molecule in the solid.

stant $F$ reduced by a fraction $\alpha$ from that of Eq. (4), to reduce the gap while leaving the spread of occupied levels nearly unchanged, combined with a proper accounting for electron-hole correlation effects neglected in the calculation, should restore satisfactory agreement, as it did in the case of Se.[9]

The calculation of Gibbons discussed by Cook and Spear[1] gave occupied molecular orbitals in $S_8$ consisting of overlapping $\pi$ and $\pi^*$ bands about 1 eV in over-all width and a narrower $\sigma$ level lying about 5 eV below the $\pi$-$\pi^*$ band. It is apparent that this description of the occupied levels does not agree with the experimental distribution of Fig. 6. In particular, no sharp isolated $\sigma$ level is found.

### C. Comparison of photoemission and optical measurements

The calculation of Gibbons was employed by Cook and Spear[1] to determine the origins of the structures in the measured $\epsilon_2(E)$ curve, which is reproduced in Fig. 7. Because the valence density of states does not have the structure calculated by Gibbons, that calculation cannot be used to evaluate the $\epsilon_2(E)$ structure.

One might try to reproduce $\epsilon_2(E)$ from the measured valence-band density of states by supposing a final-state density which is zero within the 4-eV energy gap above the valence-band maximum, and constant at higher energy. But since the peaks (1) and (4) in $\epsilon_2(E)$ are separated by 8 eV, while peaks 1 and 4 in the valence band are separated by only 4.6 eV, it is obvious that such an attempt would be unsuccessful. Consequently, a final density of states similar to that employed by Cook and Spear, which has two conduction-band levels separated by about 2.5 eV, must be supposed.

We see that the empty molecular orbitals 25 and 26 are separated by about 2.5 eV from the center of the group of orbitals 27–32 shown in Fig. 5. Thus these levels do produce a final density of states similar to that required to obtain $\epsilon_2(E)$ from the measured valence band density, if the entire group is shifted downward by 3.0 eV as proposed in Sec. IV B.

The dielectric function $\epsilon_2(E)$ is related to the joint density of initial and final states $dN/dE_{ij}$ by[19]

$$\epsilon_2(E) \approx \left(\frac{h^2e^2}{mE}\right) \sum_{i,f} f_{ij} \frac{dN}{dE_{ij}} \quad , \quad E = E_{ij} \tag{5}$$

where $f_{ij}$ is the average oscillator strength for the interband transition $i \rightarrow j$. As a first approximation we may see what sort of agreement is obtained with the assumption that $f_{ij}/E$ is constant and the final density of states is $\delta(E_F - E_1) + \delta(E_F - E_2)$, with $E_1 = 4.4$ eV and $E_2 = 6.9$ eV relative to the center of peak 1. The lower dashed line of Fig. 7 gives the part of $\epsilon_2(E)$ obtained from transitions to the lower final state and the lower thin solid line gives that obtained from transitions to the upper final state. In this crude approximation the observed peak structures are reproduced fairly well, but the relative amplitudes are in error, particularly for peak (3).

As a slightly more refined calculation the empty orbitals of Fig. 5 are shifted downward by 3.0 eV. Each occupied state is broadened to a Gaussian of width 0.6 eV and each empty state is taken to be a $\delta$ function. The sum of Eq. (5) is taken with $f_{ij}/E$ constant and the selection rules required by molecular symmetry included. The curves which result are shown in Fig. 7 for the electric vector parallel and perpendicular to the molecular $z$ axis (parallel to the normal to the molecular plane). Unfortunately, this calculation actually gives poorer agreement with the experimental curve, when the two different polarizations are summed. The dot-dashed curve of Fig. 7 was obtained by including all transitions, both allowed and forbidden, in the sum of Eq. (5). Agreement with the experimental $\epsilon_2(E)$ is better than for the sum of parallel and perpendicular components alone, which suggests that the selection rules in the solid are modified

from those of the isolated molecule, as one might anticipate. While this calculated curve is not in perfect accord with the experimental $\epsilon_2$ curve, the main elements of the structure are present at approximately the correct energies.

The $\epsilon_2(E)$ curve of Cook and Spear must be regarded as tentative since it is based on measurements using unpolarized light, although orthorhombic sulfur is optically anisotropic. Polarized-light measurements which have recently been made by Emerald *et al.*[20] exhibit definite differences from the data of Cook and Spear. In particular, peak (3) is smaller, while peaks (1) and (2) of Fig. 7 are larger than found by Cook and Spear. More definitive tests of theoretical models will be possible when these polarization-dependent spectra become available.

### D. Nature of observed valence states

An attempt was made by Gusatinskii and Nemnonov[12] to obtain the density of states of sulfur by analysis of x-ray emission spectra. They argued that dipole selection rules imply that the x-ray intensity emitted in transitions from the valence band to the $K$ shell arises from valence states of $p$ symmetry, while the x-ray intensity emitted in transitions from the valence band to the $L$ shell arises from valence states of $s$ symmetry. The $K$ emission spectrum of sulfur has three peaks corresponding in energy to those labeled 1, 3, 4 in Fig. 6, and the relative intensities are similar. The small peak 2 was not seen. In addition the $L_{II,III}$ emission spectrum consists of a broad peak about 8 eV wide with the maximum lying 12 eV below peak 1 of Fig. 6. The very weak peak at about this energy in the 21.2-eV EDC of Fig. 2 is much smaller than the $s$ valence-state peak shown by the x-ray emission spectra. Furthermore, the variation from sample to sample suggests that it is more likely due to small surface contamination than to intrinsic valence states.

While no x-ray photoemission results have been reported for sulfur, these x-ray emission results together with the x-ray photoemission results on Se and Te (Ref. 11) give one every reason to believe that a similar peak will be found in sulfur.[21] How can this extra peak in the chalcogen densities of states be understood? The simple idea of Kastner that it is due simply to atomic $s$ states must be abandoned because the great width indicates considerably interaction of adjacent atoms as does the sulfur-sulfur bond angle. However, the band-structure calculations of Sandrock[22] and of Rudge *et al.*[23] for Se do indicate a broad triplet band at about the correct energy to explain the low-lying peak in Se. On the other hand, Chen[9] was able to reproduce the structure seen in the 21.2-eV photoemission curves[8] by his molecular-orbital (MO) calculations which include all six valence electrons per atom. And we have seen that the 21.2-eV density of states of sulfur is also in excellent agreement with the MO calculation.

There are two possibilities. (i) The x-ray density of states is the correct one. In this case an explanation for the good agreement of MO calculations with the upper part of the band, and for the absence of the deeper peak from the 21.2-eV photoemission data, must be found. (ii) The six valence electrons of the chalcogens are included in the structure seen in the 21.2-eV photoemission data, and calculated by Chen. In this case the deeper peak in the x-ray photoemission data must be understood, and the calculations of Sandrock and of Rudge *et al.* must be faulty. Possibility (i) implies that optical transitions up to a photon energy greater by the energy gap of the semiconductor than the width of the upper part of the valence band should include 4 electrons/atom, while (ii) implies 6 electrons/atom.

One technique which has been used with success to determine the number of electrons participating in optical transitions is the $n_{eff}$ sum rule,[24] based on the integral

$$\int_0^{\omega_0} \omega\, \epsilon_2(\omega)\, d\omega = (2\pi^2 Ne^2/m)\, n_{eff} \,. \tag{6}$$

Employing this sum rule, Cook and Spear[1] found that $n_{eff} = 2.2$ at 14 eV for sulfur. Such a low value is inconsistent with the interpretation in their work or in the present paper of the $\epsilon_2$ data they obtained, since at 14 eV the valence band consisting of the six $3s$ and $3p$ electrons of sulfur should be exhausted. This discrepancy gives further support to the suggestion in Sec. IV C that the $\epsilon_2$ curve of Cook and Spear is not entirely correct. But it prevents obtaining an answer to the present question. In the case of Se, calculations[25] give $n_{eff} = 4$ at 12–14 eV, a result which could be consistent with either the density of states of Chen, or those of Sandrock and of Rudge *et al.* It should be noted, however, that the $n_{eff}$ curve for Se is still rising rapidly at 12 eV and might very well saturate at a value higher than 4. For example, Phillip and Ehrenreich[24] found that $n_{eff}$ for Si was only 3.5 at 16-eV photon energy although the entire valence band of 4 electrons/atom is included at this energy; hence $n_{eff} = 4$ in Se suggests that more than 4 electrons/atom are present. However, it must be admitted that the $n_{eff}$ sum rule gives somewhat ambiguous results with the chalcogens, and further considerations are needed to positively decide between the two possible valence structures.

Shevchik *et al.*[11] have argued that the x-ray photoemission results are correct and that the absence of the low-lying peak in the 21.2-eV data is due to a low final-state density. This cannot be the expla-

nation, however, because the photoemission data for $\hbar\omega$ to 10.8 eV give no final-state-density effect in Se (Ref. 8) or in sulfur (except for the 0.7-eV peak discussed earlier). Furthermore, they find for Se a considerable reduction of the low-lying peak amplitude at 40.8-eV photon energy, relative to the x-ray photoemission result, although the final-state-density effect should be negligible. Supposing that the low-lying peak is due to states of $s$ symmetry while the upper valence band is primarily $p$ symmetry, one might argue for a matrix-element effect. However, in the cases of Si and Ge x-ray emission spectra[26] indicate that the lower part of the valence band is $s$-like, just as in S, but the photoemission densities of states at 21.2 eV and at higher energies are essentially identical,[27] in contrast with the chalcogens. Because of these considerations only a complete calculation of the expected photoemission results using the band structures and wave functions of Rudge *et al.*, including transition strengths at various photon energies, and agreement with the observed density of states at all photon energies, should be regarded as conclusively establishing the origin of the deeper peak present in the higher-energy photoemission data.

If possibility (ii) is to be accepted some explanation for the lower-lying peak observed in x-ray photoemission is needed. Because this lower peak has the same general shape as the upper valence structure[11]—it is a doublet with about the same peak spacing as that of the upper valence band—one possible explanation is that it is a replica of the upper band shifted by an energy loss of 10 eV. The surface-plasmon energy of[27] $E_{sp} = E_{bp}/\sqrt{2}$, where the bulk plasmon energy $E_{bp} \approx 19$ eV for Se,[11] is at approximately the correct energy. Furthermore, Mahan[28] has calculated that the probability that an escaping photoexcited electron should create one surface plasmon is near 1. But if this explanation is to be accepted a reason for the much smaller amplitude of the surface-plasmon energy-loss peak in the $3d$ energy-loss spectrum[11] must still be found.

The molecular-orbital calculations for sulfur and selenium (with one parameter adjusted) give excellent agreement with these 21.2-eV photoemission data; the value of $n_{eff}$ for selenium also favors the idea that all six valence electrons are included in the 21.2-eV density-of-states curves. Therefore the possibility that the six valence electrons of the chalcogens are contained in the valence band found in these measurements is at least as reasonable as the alternative. Further calculations are needed before conclusive rejection of one configuration or the other will be justified.

## ACKNOWLEDGMENTS

I wish to thank I. Chen for his permission to use unpublished calculations, and for the level-broadening computer program, and G. B. Fisher, R. Zallen, M. Slade, and G. Lucovsky for valuable discussions.

[1]B. E. Cook and M. E. Spear, J. Phys. Chem. Solids 30, 1125 (1969).
[2]F. G. Hellyer, Ph.D. thesis (University of Leicester) (unpublished).
[3]R. J. Komp and T. J. Fitzsimmons, J. Photochem. Photobiol. 8, 419 (1968).
[4]I. Chen, Phys. Rev. B 2, 1053 (1970).
[5]I. Chen, Phys. Rev. B 2, 1060 (1970).
[6]R. J. F. Dalrymple and W. E. Spear, J. Phys. Chem. Solids 33, 1071 (1972).
[7]M. Kastner, Phys. Rev. Lett. 28, 355 (1972).
[8]P. Nielsen, Phys. Rev. B 6, 3739 (1972).
[9]I. Chen, Phys. Rev. B 7, 3672 (1973).
[10]R. A. Pollack, S. Kowalczyk, L. Ley, and D. A. Shirley, Phys. Rev. Lett. 29, 274 (1972).
[11]N. J. Shevchik, M. Cardona, and J. Tejeda, Phys. Rev. B 8, 2833 (1973).
[12]A. N. Gusatinskii and S. A. Nemnonov, Fiz. Tverd. Tela 11, 1528 (1969) [Sov. Phys.-Solid State 11, 1241 (1969)].
[13]R. E. Honig, RCA Rev. 18, 195 (1957).
[14]Material supplied by R. H. Zallen and M. L. Slade.
[15]J. Berkowitz, in *Elemental Sulfur*, edited by B. Meyer (Wiley, New York, 1965), p. 152.
[16]M. Thackray, in *Elemental Sulfur*, edited by B. Meyer (Wiley, New York, 1965), p. 152.
[17]C. N. Berglund and W. E. Spicer, Phys. Rev. 136, A1030 (1964).
[18]L. E. Lyons, J. Chem. Soc. (Lond.) 5001 (1957).
[19]J. C. Phillips, in *Solid State Physics*, edited by F. Seitz and D. Turnbull (Academic, New York, 1966), Vol. 18, p. 55.
[20]R. L. Emerald, R. E. Drews, and R. Zallen (unpublished).
[21]G. B. Fisher has indeed seen such structure in ESCA measurements on S (private communication).
[22]R. Sandrock, Phys. Rev. 169, 642 (1968).
[23]W. E. Rudge, C. D. Chekroun, and I. B. Ortenburger, Bull. Am. Phys. Soc. 18, 350 (1973).
[24]H. R. Phillip and H. Ehrenreich, Phys. Rev. 129, A1550 (1963).
[25]P. Nielsen, M. Slade, and R. Zallen (unpublished), based on $\epsilon_2$ data of A. Leiga, J. Opt. Soc. Am. 58, 1441 (1968), and of P. Bammes, R. Klucker, and E. E. Koch, Phys. Status Solidi B 49, 561 (1972).
[26]G. Wiech, in *Soft X-Ray Band Spectra and the Electronic Structure of Metals and Materials*, edited by D. J. Fabian (Academic, New York, 1968), p. 59.
[27]W. D. Grobman and D. E. Eastman, Phys. Rev. Lett. 29, 1508 (1972).
[28]G. D. Mahan, Phys. Status Solidi B 55, 703 (1973).
[29]D. J. Gibbons, Mol. Cryst. Liq. Cryst. 10, 137 (1970).